Electronic Supplementary Material (ESI) for Journal of Materials Chemistry A.

Electronic Supplementary Information

General strategy for coating metal-organic frameworks on diverse components and architectures

Gang Huang,[ab] Dongming Yin[ab] and Limin Wang[c]*

[a]State Key Laboratory of Rare Earth Resource Utilization, Changchun Institute of Applied Chemistry, Chinese Academy of Sciences, Changchun, 130022, P. R. China

[b]University of Chinese Academy of Sciences, Beijing, 100049, P. R. China

*To whom correspondence should be addressed. Email: lmwang@ciac.ac.cn

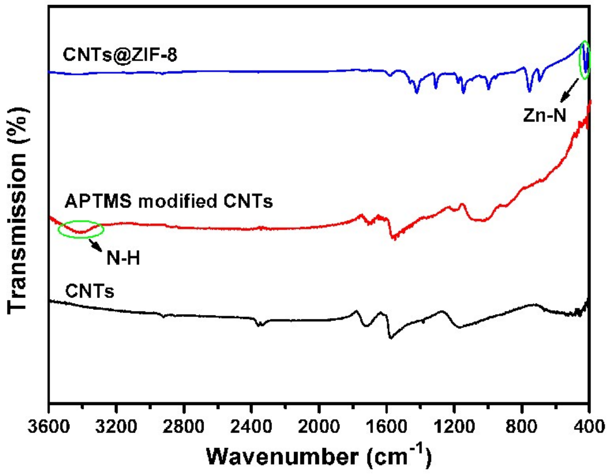

Fig. S1 FTIR spectra of the untreated CNTs, APTMS modified CNTs and core@shell CNTs@ZIF-8 (fractured) nanowires.

As can be seen in the FTIR spectra (Fig. S1, ESI), a new broad band in the range of 3200–3600 cm^{-1} emerges after APTMS modification, which is ascribed to the N–H stretching and confirms the amination of core components with APTMS treatment.

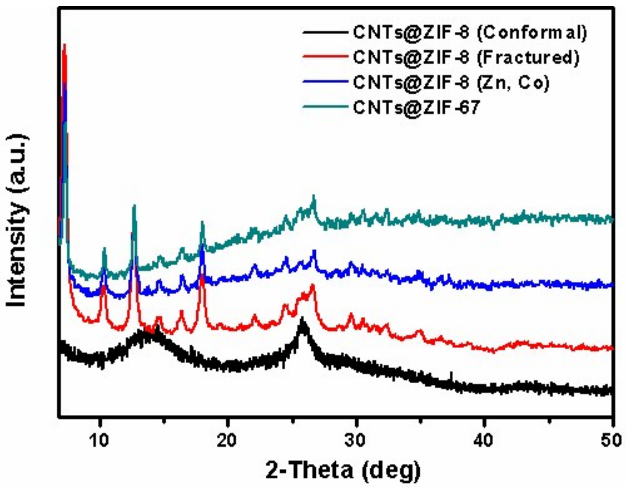

Fig. S2 XRD patterns of the as-synthesized core@shell products.

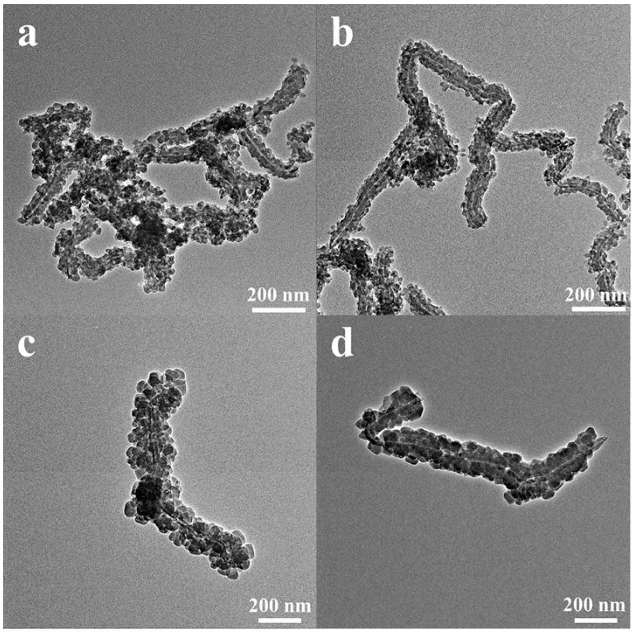

Fig. S3 TEM images of (a and b) CNTs@ZIF-8-0.5 (fractured) and (c and d) CNTs@ZIF-8-2 (fractured) nanowires.

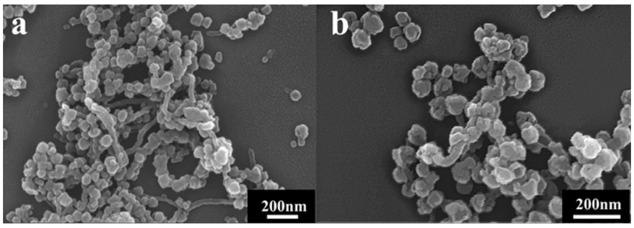

Fig. S4 SEM images of CNTs@ZIF-8 prepared without PSS treatment.

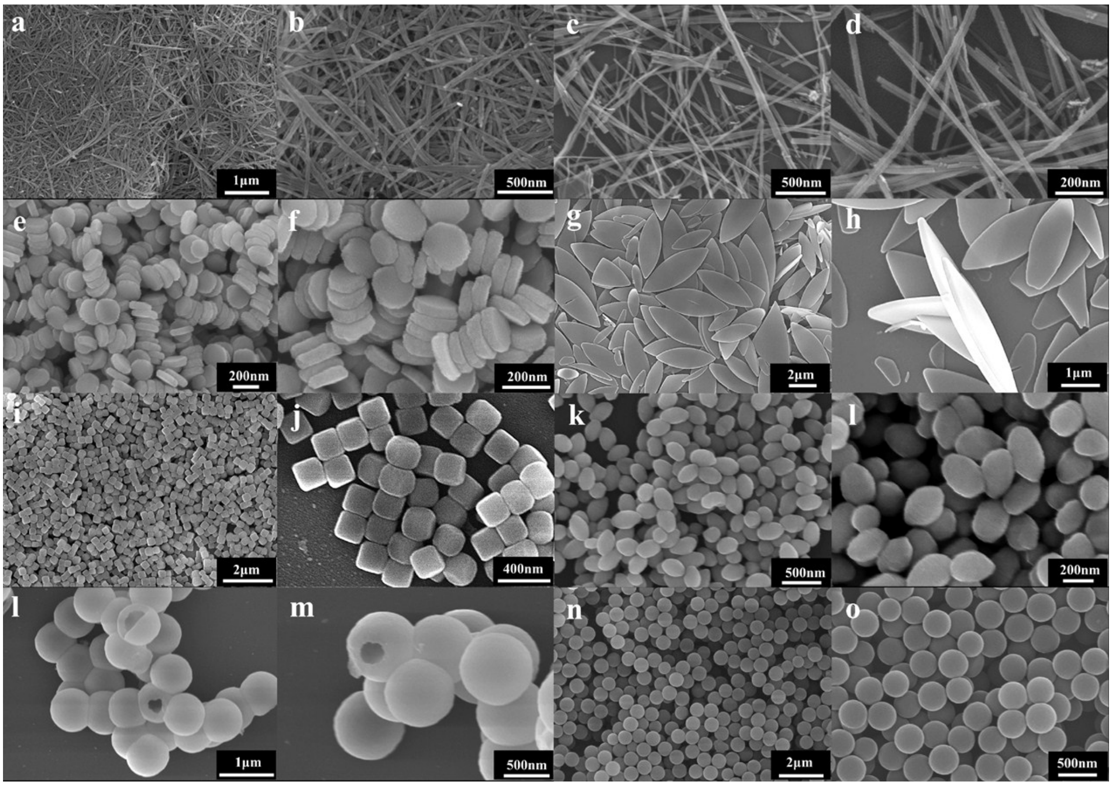

Fig. S5 SEM images of the diverse core components. (a and b) $Ni(OH)_2$ nanowires; (c and d) $LiMn_2O_4$ nanowires; (e and f) Fe_2O_3 nanoplates; (g and h) ZIF-L leaf-like microplates; (I and j) $Ni_3[Co(CN)_6]_2$ nanocubes; (k and l) Fe_2O_3 nanospindles; (l and m) SiO_2 hollow nanospheres and (n and o) RF nanospheres.

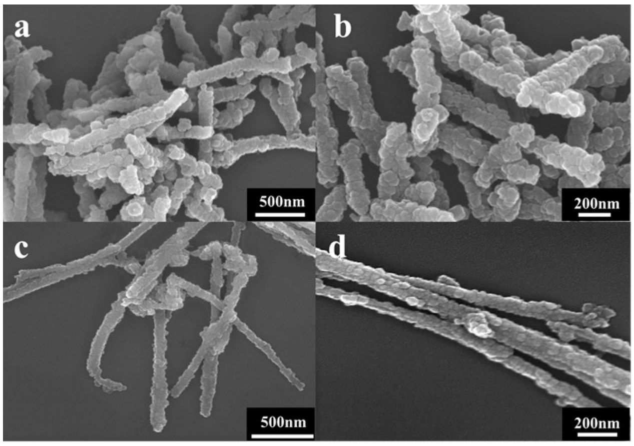

Fig. S6 SEM images of (a and b) $Ni(OH)_2$@ZIF-8 and (c and d) $LiMn_2O_4$@ZIF-8 nanowires.

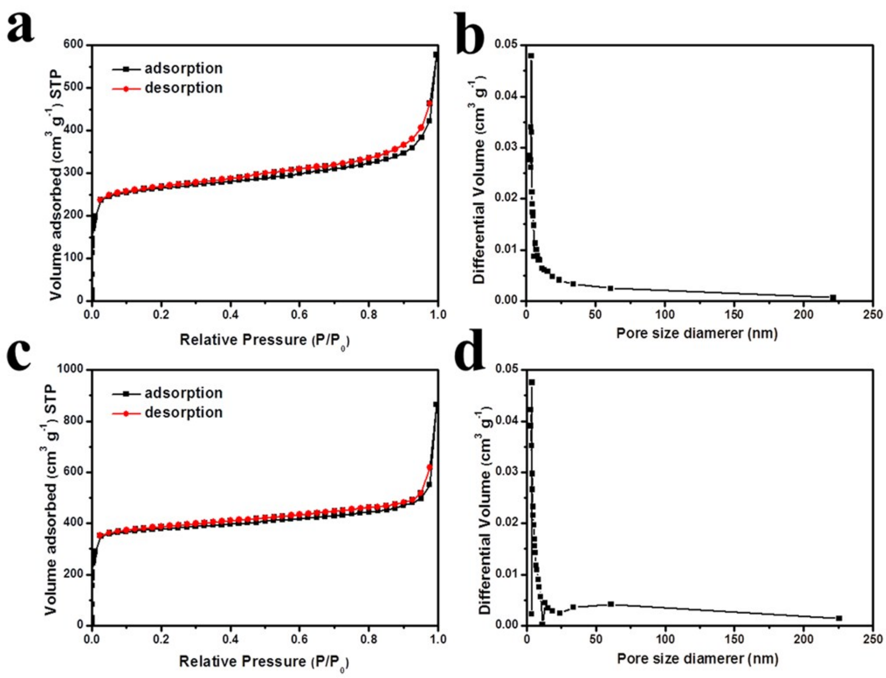

Fig. S7 N_2 adsorption-desorption isotherms and the corresponding pore size distributions of (a and b) CNTs@ZIF-8 (fractured) nanowires and (c and d) $Ni(OH)_2$@ZIF-8 nanowires.

N_2 sorption isotherms of the CNTs@ZIF-8 (fractured) and $Ni(OH)_2$@ZIF-8 nanowires are shown in Fig. S7. The observed features of the isotherms resemble type I and IV isotherms with a H3 type hysteresis loop. The sharp uptakes at low pressure imply the presence of micropores from ZIF-8. The distinct hysteresis in the relative pressure region of P/P_0>0.3 underscores the mesopores characteristics, which may arise from the void space between the interconnected nanosized building blocks of fractured shell. The BET surface areas of CNTs@ZIF-8 (fractured) and $Ni(OH)_2$@ZIF-8 are 1055.8 and 1592.7 m^2 g^{-1}, respectively. Calculated from the desorption branch using the BJH modal, the average pore size distributions of CNTs@ZIF-8 (fractured) and $Ni(OH)_2$@ZIF-8 center at 3.705 and 3.715 nm.

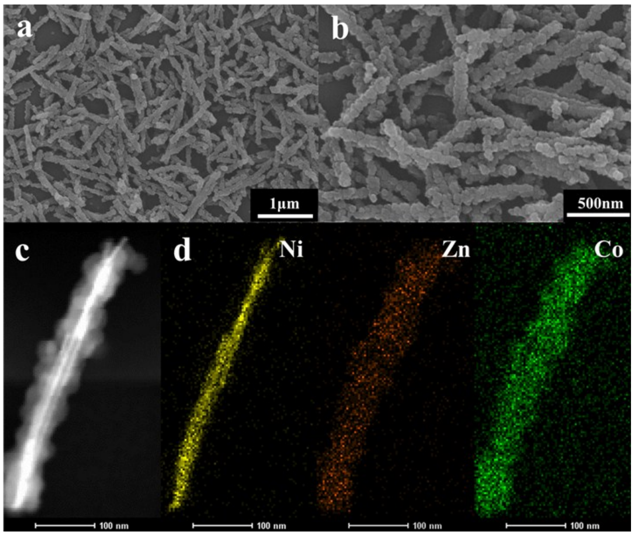

Fig. S8 (a and b) SEM images, (c) HAADF-STEM image and (d) elemental mapping of $Ni(OH)_2$@ZIF-8 (Zn, Co) nanowires.

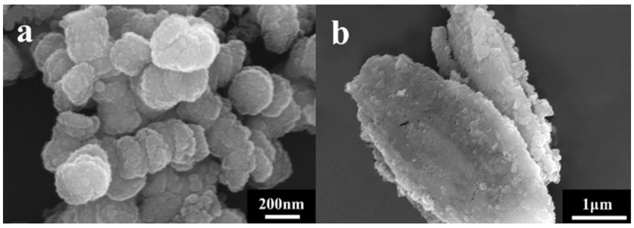

Fig. S9 SEM images of (a) Fe_2O_3@ZIF-8 nanoplates and (b) ZIF-L@ZIF-8 microplates.

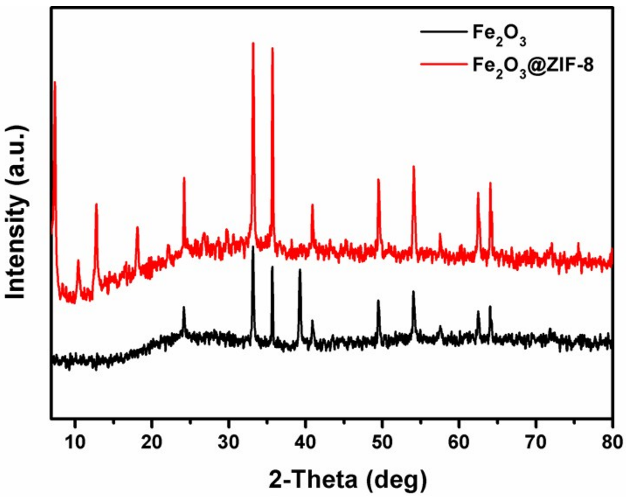

Fig. S10 XRD patterns of Fe_2O_3 and Fe_2O_3@ZIF-8 nanoplates.

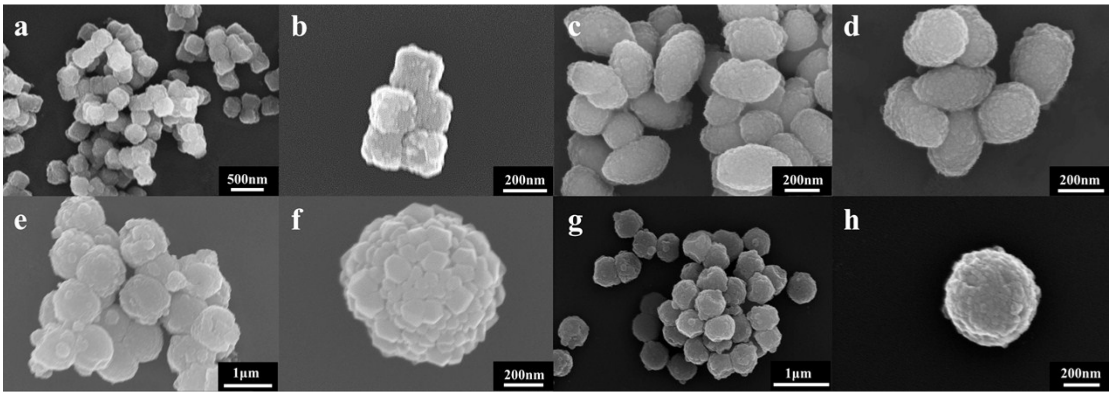

Fig. S11 SEM images of 3D core@shell composites. (a and b) $Ni_3[Co(CN)_6]_2$@ZIF-8 nanocubes; (c and d) Fe_2O_3@ZIF-8 nanospindles; (e and f) SiO_2@ZIF-8 hollow nanospheres and (g and h) RF@ZIF-8 nanospheres.

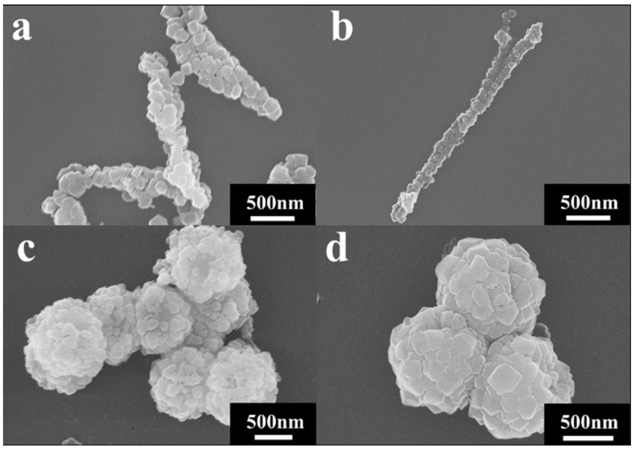

Fig. S12 SEM images of (a) $Ni(OH)_2$@ZIF-67 nanowires; (b) $LiMn_2O_4$@ZIF-67 nanowires; (c) SiO_2@ZIF-67 hollow nanospheres and (d) RF@ZIF-67 nanospheres.

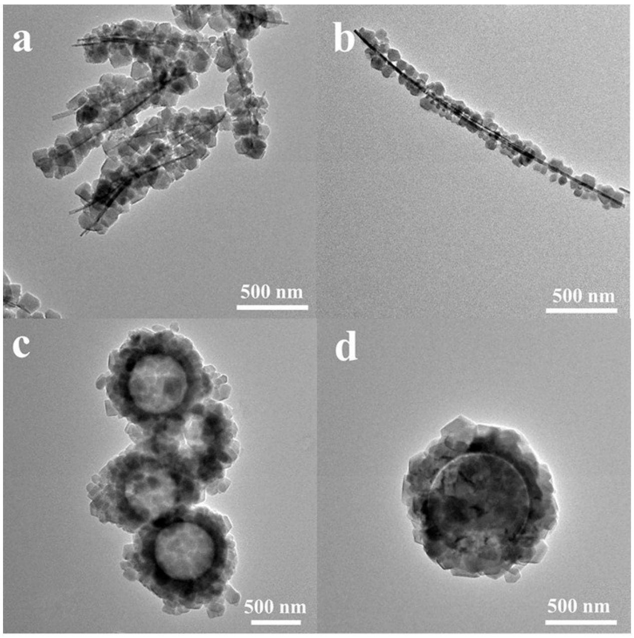

Fig. S13 TEM images of (a) $Ni(OH)_2$@ZIF-67 nanowires; (b) $LiMn_2O_4$@ZIF-67 nanowires; (c) SiO_2@ZIF-67 hollow nanospheres and (d) RF@ZIF-67 nanospheres.

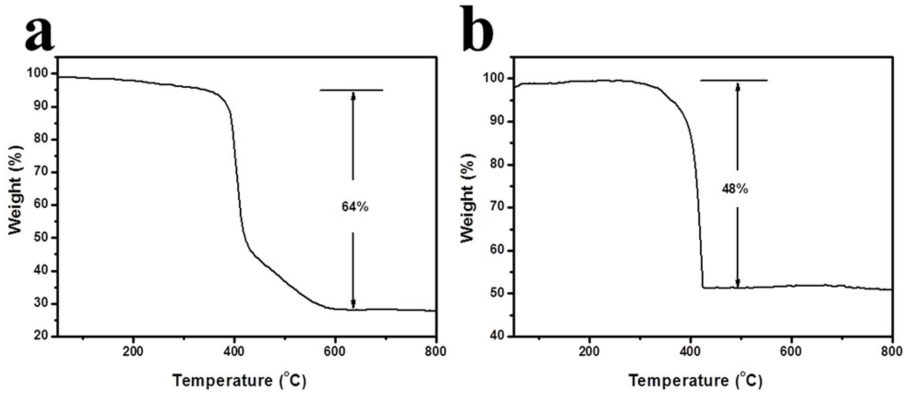

Fig. S14 Thermogravimetric analysis curves of (a) CNTs@ZIF-8 (Zn, Co) and (b) $Ni(OH)_2$@ZIF-8 (Zn, Co) nanowires.

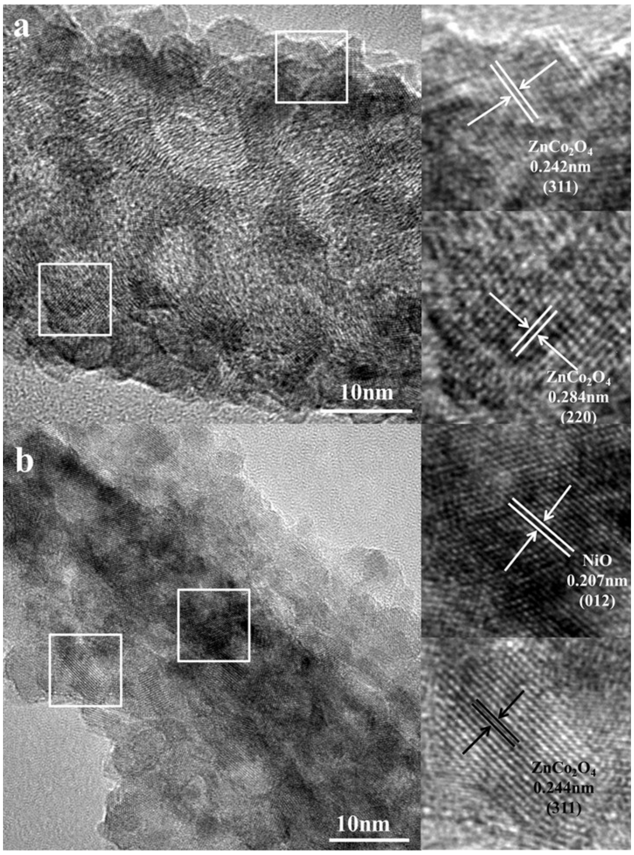

Fig. S15 HRTEM images of (a) CNTs@$ZnCo_2O_4$ and (b) NiO@$ZnCo_2O_4$ nanowires.

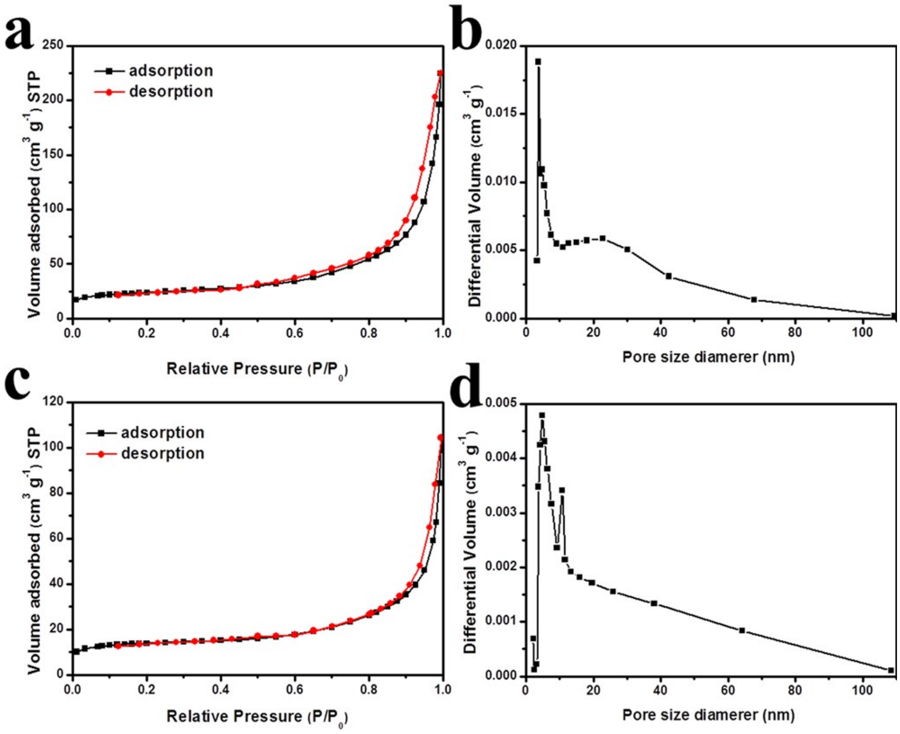

Fig. S16 N_2 adsorption-desorption isotherms and the corresponding pore size distributions of (a and b) CNTs@$ZnCo_2O_4$ and (c and d) NiO@$ZnCo_2O_4$ nanowires.

Table S1 The diameter and shell thickness of core@shell CNTs@ZIF-8 (fractured) nanowires synthesized at different precursor's concentrations

	CNTs@ZIF-8-0.5 (fractured)	CNTs@ZIF-8 (fractured)	CNTs@ZIF-8-2 (fractured)
Diameter	66 nm	76 nm	156 nm
Shell thickness	20 nm	26 nm	65 nm

Table S2 Summary of representative anode materials for Li-ion batteries

Anode materials	Cycling performance	Rate capability	Ref.
Peapod-like Co_3O_4@Carbon nanotube arrays	700 mA h g^{-1} after 100 cycles at 100 mA g^{-1}	453 mA h g^{-1} at 1000 mA g^{-1}	1
Two-dimensional porous micro/nano NiO	568 mA h g^{-1} after 50 cycles at 200 mA g^{-1}	300 mA h g^{-1} at 1000 mA g^{-1}	2
ZnO-loaded/porous carbon composite	654 mA h g^{-1} after 100 cycles at 100 mA g^{-1}	497 mA h g^{-1} at 1000 mA g^{-1}	3
Porous Co_3O_4/CuO composite	839 mA h g^{-1} after 150 cycles at 100 mA g^{-1}	700 mA h g^{-1} at 1000 mA g^{-1}	4
Carbon nanofibers anchored with $Zn_xCo_{3-x}O_4$ nanocubes	600 mA h g^{-1} after 300 cycles at 500 mA g^{-1}	337 mA h g^{-1} at 1000 mA g^{-1}	5
Porous polyhedral $ZnCo_2O_4$/CNTs composites	864.6 mA h g^{-1} after 150 cycles at 100 mA g^{-1}	606 mA h g^{-1} at 2000 mA g^{-1}	6
Hierarchical $ZnCo_2O_4$/NiO core/shell nanowire arrays	357 mA h g^{-1} after 50 cycles at 100 mA g^{-1}	200 mA h g^{-1} at 800 mA g^{-1}	7
CNTs@$ZnCo_2O_4$ nanowires	750 mA h g^{-1} after 100 cycles at 100 mA g^{-1}	460 mA h g^{-1} at 1000 mA g^{-1}	This work
NiO@$ZnCo_2O_4$ nanowires	1002 mA h g^{-1} after 100 cycles at 100 mA g^{-1}	462 mA h g^{-1} at 1000 mA g^{-1}	

Reference

1. D. Gu, W. Li, F. Wang, H. Bongard, B. Spliethoff, W. Schmidt, C. Weidenthaler, Y. Y. Xia, D. Y. Zhao and F. Schuth, *Angew. Chem. Int. Ed.*, 2015, **127**, 7166.
2. H. L. Cao, X. F. Zhou, C. Zheng and Z. P. Liu, *ACS Appl. Mater. Interfaces,* 2015, **7**, 11984.
3. X. Y. Shen, D. B. Mu, S. Chen, B. R. Wu and F. Wu, *ACS Appl. Mater. Interfaces*, 2013, **5**, 3118.
4. Q. Hao, D. Y. Zhao, H. M. Duan and C. X. Xu, *ChemSusChem*, 2015, **8**, 1435.
5. R. Z, Chen, Y. Hu, Z. Shen, Y. L. Chen, X. He, X. W. Zhang and Y. Zhang, *ACS Appl. Mater. Interfaces*, 2016, **8**, 2591.
6. Q. Ru, X. Song, Y. Mo, L. Guo and S. Hu, *J. Alloys Com*., 2016, **654**, 586.
7. Z. Sun, W. Ai, J. Liu, X. Qi, Y. Wang, J. Zhu, H. Zhang and T. Yu, *Nanoscale*, 2014, **6**, 6563.